

## The impact of parasitic capacitances on the accuracy of scale transformation of high-voltage dividers

**Purpose.** The aim of this work is the determination of the parasitic capacitance's influence on the accuracy of scale transformation of high-voltage dividers. Analyzing the possibilities of reducing such influence is a pressing **problem** for high voltage measurement, especially at high frequency range of input voltage. **Methodology.** Mathematical modeling of the voltage divider equivalent circuit, considering parasitic capacitances and inductances has been performed in the QUCS circuit simulator software under sinusoidal alternating current conditions in the range from 100 Hz to 1 MHz. Using the FEMM software, the finite element method was used to simulate the density distribution of capacitive currents in the module with capacitance graded insulation of the high-voltage arm of the voltage divider. **Results.** The results of the calculations show that the percentage of parasitic capacitive currents decreases exponentially depending on the ratio of the outer radii of the shielding disks to the distance between them. However, even with the outer radii of the shielding disks of about 3 m, capacitive currents still make up about 1 % of the total current flowing in the measuring circuit of the voltage divider. Instead of increasing outer radii, it is proposed to use high-voltage capacitance graded insulation between the shielding disks. As a result, a stable error of large-scale voltage transformation was obtained when the values of parasitic capacitances change, and it is proposed to manufacture the high-voltage arm of the voltage divider from the same type of high-voltage modules. **Originality.** The results of modeling the dependence of the accuracy of the voltage divider scale transformation on the ratio of the structural elements geometric parameters of its high-voltage arm were obtained. The solution has been proposed that involves changing the design of the high-voltage arm of the voltage divider, which significantly reduces the dependence of its scale transformation error on significant changes in the parasitic capacitances of the structure components on grounded surfaces. **Practical value.** The results of mathematical modeling of the characteristics of the voltage divider high-voltage arm make it possible to design, for the purpose of serial production, the same type of high-voltage modules for assembling on-site broadband voltage dividers for any nominal voltage, which will have the possibility of integration into Smart Grid systems. References 23, tables 1, figures 8.

**Key words:** high-voltage divider, parasitic capacitances, scale transformation accuracy.

В роботі розглянуто вплив будови високовольтного плеча подільника напруги на його характеристики. Для забезпечення зменшення впливу паразитних ємностей конструктивних елементів на зосереджені елементи активної частини та на зовнішні об'єкти досліджено методи екранування зосереджених елементів. Математичним моделюванням визначено вплив співвідношення геометричних параметрів конструкційних елементів високовольтного плеча на похибку масштабного перетворення напруги в області високих частот. В результаті моделювання обрано спосіб екранування зосереджених елементів активної частини подільника напруги з використанням багатошарової ізоляції конденсаторного типу, яка забезпечує стабільність похибки масштабного перетворення напруги в широкому діапазоні частот. Запропоновані зміни в будові високовольтного плеча дозволяють перейти на модульну будову подільника напруги і перейти до його серійного виробництва. Бібл. 23, табл. 1, рис. 8.

**Ключові слова:** високовольтний подільник напруги, паразитні ємності, точність масштабного перетворення.

**Problem definition.** High-voltage dividers are common large-scale voltage converters used in both microelectronics and high-voltage test and research laboratories. However, these electrical devices are not widely used in the power industry, in particular, in high-voltage electrical installations, since their structure does not allow getting rid of a number of disadvantages that complicate their integration into analog or digital substations as broadband large-scale high-voltage converters [1]. For example, under laboratory conditions, large-scale voltage conversion errors in a wide frequency range of the order of 0.1 are obtained for high-voltage dividers, however, the structure of such a voltage divider is complex and not suitable for wind loads, precipitation, and temperature changes. In open switchgears, the presence of objects near the voltage divider that are at a different potential (or grounded) significantly affect the parasitic capacitances of its high-voltage arm. Parasitic capacitances on such objects significantly affect the accuracy of large-scale voltage conversion at high frequency. Also, the temperature dependence of the complex resistances of the lumped elements of the high-voltage arm affects the scaling factor of the voltage divider. In addition, the production of high-voltage dividers for the specific tasks of the customer complicates the creation of a unified system of mass production of such equipment. This limits the possibility to significantly improve the determination of power quality indicators, safety and automation of processes at high-voltage facilities. For these and other reasons, high-voltage dividers have not yet been used as large-scale high-

voltage converters in a wide frequency range. They could not replace, even partially, the existing electromagnetic voltage transformers at high-voltage substations. This applies, in particular, to the determination of power quality indicators, some of which are significantly distorted by the electromagnetic cores of transformers.

**Analysis of publications on research topic.** The simplest high-voltage divider consists of two serially connected sections of a circle of lumped elements: high-voltage and low-voltage arms. Each of the arms is a section consisting of one or more series-connected lumped elements (the structure of the low-voltage arm can be significantly different, depending on the purpose of the voltage divider) [1, 2]. The principle of voltage division is that the total voltage to be proportionally distributed is applied to the series-connected arms of the voltage divider and is distributed among the lumped elements in proportion to their complex resistances. This principle of voltage distribution is used both for functional voltage distribution (for example, in high-voltage air circuit breakers for ultra-high voltages to divide a long electric arc into a number of short arcs in order to extinguish them more efficiently), and for the purpose of measuring high voltage by connecting measuring devices in parallel to the circuit low-voltage arm.

For measuring high voltage, the high-voltage arm of the voltage divider must consist not only of a link of lumped elements of the active part, but also of high-voltage insulation and armature that holds these lumped elements. High-voltage insulation and armatures

practically do not affect the measurement of constant voltage, accordingly, for measuring high constant voltage, it is sufficient to provide the high-voltage and low-voltage arms of the voltage divider with high-quality precision lumped elements (resistors) that will provide the necessary scaling factor, in accordance with the formula:

$$K_d = \frac{U}{U_{LV}} = \frac{R_{HV} + R_{LV}}{R_{LV}} = 1 + \frac{R_{HV}}{R_{LV}}, \quad (1)$$

where  $U$  is the measured high voltage;  $U_{LV}$  is the voltage on the low-voltage arm;  $R_{HV}$  is the total active resistance of the area of lumped elements of the high-voltage arm;  $R_{LV}$  is the total active resistance of the lumped elements of the low-voltage arm.

However, if the voltage divider is used to measure voltage that changes with time (sinusoidal voltage, transients, etc.), the structure of the arms of the voltage divider becomes significantly more complicated. In AC circuits, especially, with an increase in the frequency or rapidity of transient processes, the influence of reactive component elements of electric circuits increases [2–4]. It is necessary to take into account not only the voltage distribution between the lumped elements of the arms of the voltage divider, but also the parasitic capacitances and inductances, which are integral components of any lumped elements of the electric circuit, as well as the components of the structural elements of its arms. In modern high-voltage dividers designed for measuring alternating voltage and transients (broadband voltage dividers), the structure of high-voltage insulation and armature form complex systems of parasitic capacitances on nearby lumped elements, on grounded structural elements and nearby objects that are under a different potential. In modern designs of voltage dividers, the method of shielding the lumped elements of the high-voltage and low-voltage arms is used in order to reduce the influence of parasitic capacitances on the voltage distribution between different sections of the general electric circuit of the active part. Large-sized capacitive screens are also used, designed to regulate the distribution of the electric field. In works [4–10], various design solutions for the structure of the high-voltage arm of the voltage divider are proposed, which allow to partially reduce the influence of parasitic capacitances (up to a certain level of input voltage frequencies). As a rule, parallel shielding conductive disks are used for this purpose, which between them form a distribution of the electric field that is close to uniform, and between the planes of these disks, sections of the circle of lumped elements of the active part of the voltage divider are placed, thus dividing the high-voltage circuit into a number of shielded sections. Shielding disks and support insulators form the armature that keeps the lumped elements of the high-voltage arm of the voltage divider in a certain spatial position. The consequence of such a structure is the appearance of additional parasitic capacitances (between the shielding disks), which form a high-voltage capacitive (shielding) circuit, which is parallel to the circuit of lumped elements of the high-voltage arm. The lumped circuit elements of the high-voltage arm will have parasitic capacitances on the shielding disks. The greater will be the differences in the potential distribution between the lumped elements and the shielding disks, the greater will be the parasitic capacitive currents between the lumped elements and these disks (especially at a high frequency of the applied voltage).

To analyze the influence of the structure of the high-voltage arm of the voltage divider on its frequency characteristics, researchers offer both direct measurement methods [10–15] using high-precision and reference measuring devices, as well as analytical methods or numerical modeling [15–22], which allow predicting the characteristics of designed voltage dividers or to explain the actual measured parameters for further improvement of the structure of voltage dividers.

In all the publications reviewed, the influence of parasitic capacitances of both the lumped elements of the active part and the structural components of the voltage divider structure, both on external objects and among themselves, is recognized as significant. However, recognizing the significance of the influence of parasitic capacitances on the accuracy of large-scale transformation of voltage dividers at high frequency, in the reviewed publications, researchers propose various schemes and spatial arrangement of lumped elements of the active part, without paying much attention to the structure of the shielding areas of the high-voltage arm (mainly, such studies consider the structure and spatial arrangement of high-voltage large-sized screens). Since the structure of the high-voltage arm of the voltage divider has a significant effect on the distribution of voltage on lumped elements of the active part, it is important to find design solutions that would allow combining mechanical and shielding functions in a wide frequency range.

**The goal of the work** is to analyze the structure of the high-voltage arm of the voltage divider and to identify the factors that affect the accuracy of large-scale voltage conversion in a wide frequency range in the presence of parasitic capacitances in the circuit of the high-voltage arm.

**Analysis of the structure of the high-voltage arm of the voltage divider.** To overcome the above-described consequences of the presence of parasitic capacitances between the lumped elements of the high-voltage arm and the surfaces under a different potential, there are several options for the structure of the high-voltage arm. In addition to the above-mentioned method of shielding the sections of the lumped elements of the high-voltage arm of the voltage divider with the help of conductive shielding disks, parallel circuits of lumped shielding elements are used, which are additionally placed between the shielding disks in order to increase the conductivity between them and, as a result, reduce the impact of leakage of capacitive currents from these disks on surfaces under a different potential. Both shunting with resistors and shunting with capacitors or a mixed  $RC$  connection of shielding disks are used. You can reduce the value of the active resistances of the shielding circuit only to certain limits: if the total resistance of the shielding circuit of the high-voltage arm of the voltage divider is too small, significant currents will flow through it and significant energy will be released in the form of heat, which will affect the stability of the circuit characteristics. In addition to creating an excess load on the source, such energy can cause heating not only of the lumped elements of the shielding circuit, but also of the elements of the measuring circuit, reducing the stability of these resistances.

Figure 1 shows a simplified substitution circuit of a high-voltage divider, in which the low-voltage arm is represented by one, and the high-voltage arm is represented by three series-connected high-voltage, high-resistance, low-inductance resistors of the same rating ( $R1 - R4$ ).

Parasitic inductances of these resistors are represented by elements L1 – L4. The high voltage from the source V1 is applied to the entire voltage divider, and is measured on the low-voltage arm by the meter U<sub>NN</sub>, the internal resistance of which is considered infinite in the simulation. In the absence of parasitic capacitances and the identity of resistors R1 - R4, the voltage on the low-voltage arm should, in accordance with (1), be equal to 25 % of the input voltage of the high-voltage source V1. Capacitances C1 –C4 in Fig. 1 are parasitic capacitances that occur between the shielding disks forming the sections of the voltage divider and the parallel shielding capacitive circuit. Parasitic inductances L5 – L8 are also added to these capacitors in series, which refer to the shielding capacitive circuit, if capacitors are additionally installed in this circuit between the shielding disks to increase the capacitance in this circuit. Parasitic capacitances C5 – C6 occur between the shielding disks and the high-voltage electrode (as a rule, these capacitances have very small values); parasitic capacitances C7 – C8 occur between the shielding disks and the grounded surfaces and, as a rule, have values up to units of picofarads (rarely larger). Parasitic capacitances C9 – C11 occur between the lumped elements of the measuring circuit of the voltage divider and the shielding disks of the shielding circuit. The circuit according to Fig. 1 does not take into account all the parasitic capacitances and inductances of the high-voltage divider and considers a small number of sections, but allows considering the principle relationships between the main and parasitic characteristics of both lumped and structural elements in its composition.

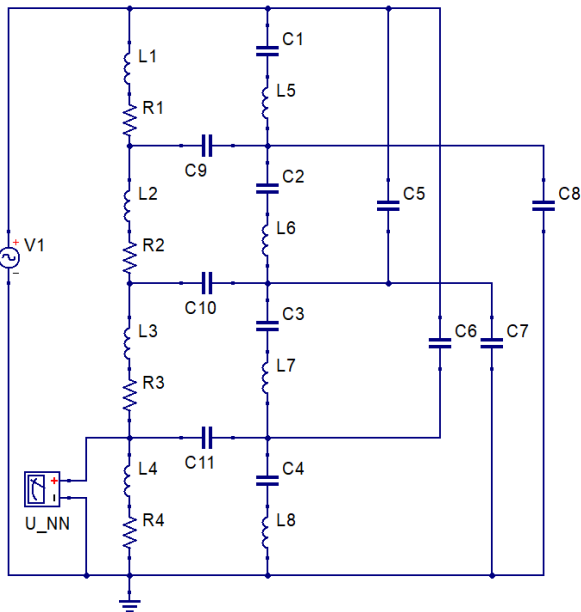


Fig. 1. Schematic substitution circuit of voltage divider taking into account parasitic capacitances and inductances

For the numerical evaluation of the characteristics of lumped and parasitic elements of the circuit in Fig. 1, the possibility of using low-power high-voltage resistors in the active part of the voltage divider is considered. As a rule, when using low-power resistors, the current in the active part is limited to the order of 1 mA. Suppose that the amplitude of the applied voltage of the source V1 is 10 kV. Accordingly, the total input resistance of the voltage divider according to Ohm law (neglecting the insignificant inductive resistances) can be roughly estimated as 10 MΩ.

Accordingly, resistors R1 – R4 will have a nominal resistance of 2.5 MΩ. Parasitic capacitances that arise between the shielding disks of the shielding part of the voltage divider circuit can be estimated approximately by formula for parallel plate capacitor:

$$C = \frac{\epsilon_0 \cdot \epsilon \cdot \pi \cdot (R_2^2 - R_1^2)}{d}, \quad (2)$$

where  $\epsilon_0$  is the electrical constant;  $\epsilon$  is the relative permittivity of the dielectric (if the dielectric is air,  $\epsilon = 1$  can be considered as an approximation);  $d$  is the distance between parallel disks;  $R_2$  is the outer radius of the shielding disk;  $R_1$  is the radius of the inner hole in the shielding disk (intended for the location of the measuring circle of lumped elements).

According to (2), if we take  $R_1 = 3$  cm,  $R_2 = 10$  cm,  $d = 1$  cm, we obtain  $C \approx 25$  pF. Parasitic inductances of resistors L1 - L4 can be taken as equal to 10 nH (for low-inductance resistors). The parasitic capacitances of the lumped elements of the measuring circuit C9 – C11 can be approximately equal to 1 pF (these capacitances are insignificant and depend on the dimensions of the resistors). Parasitic inductances L5 – L8 can be shorted in the absence of shunt capacitors between the shielding disks, or will have very little value when using pulsed capacitors (for example, PHE-450 type or similar), therefore, as a first approximation, these inductances in the circuit can be taken as 1 nH. Parasitic capacitances C5 – C6 can be determined only by mathematical modeling using numerical methods of the electrostatics problem, taking into account the specific geometry of the shielding disks. This also applies to parasitic capacitances C7 – C8. As a rule, the capacitances for the grounded surfaces are several times larger than the corresponding capacitances for the high-voltage electrode. According to the performed mathematical modeling of the problem of electrostatics in the FEMM software package for the geometry of the shielding disks used for calculations according to (2), it is possible to determine the approximate value of these capacitances:  $C5 \approx 3$  pF;  $C6 \approx 1.5$  pF;  $C8 \approx 5$  pF;  $C7 \approx 7$  pF (if the thickness of the shielding conductive disks is assumed to be equal to 5 mm).

Mathematical modeling of the electric circuit in Fig. 1 in the QUCS circuit modeling software package in the problem of sinusoidal AC in the range from 100 Hz to 1 MHz with discretization of 5000 points gives a graph of the dependence of the voltage on the low-voltage arm (Fig. 2).

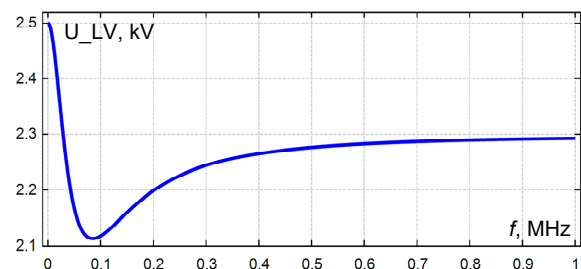


Fig. 2. Dependence of the voltage on the low-voltage arm of the voltage divider on the frequency at the capacitances in the shielding circuit of 25 pF

This graph shows the maximum deviations (in the considered frequency  $f$  range) of the output voltage  $U_{LV}$  of the voltage divider from the nominal (2.5 kV) of the order of 15 %, which is unacceptable for large-scale

conversion of high voltage for the purpose of determining power quality indicators. If the capacitance of the shielding circuit is increased to 10 nF, a similar simulation in the QUCS software package gives a graph of the dependence of the output voltage, shown in Fig. 3.

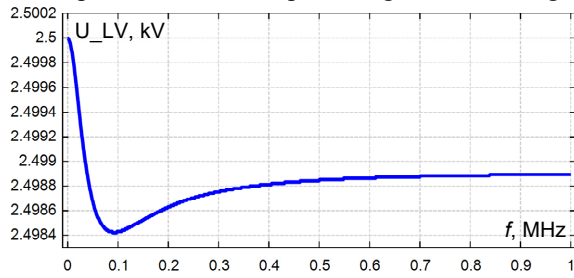


Fig. 3. Dependence of the voltage on the low-voltage arm of the voltage divider on the frequency at the capacitances in the shielding circuit of 10 nF

Analyzing the graph in Fig. 3, it can be seen that the maximum deviations of the output voltage are less than 0.1 % in the frequency  $f$  range from 1 Hz to 1 MHz, which can be considered acceptable for the use of such a voltage divider when measuring all power quality indicators at high voltage. When expanding the range of input frequencies to 50 MHz, the result of the analysis gives the graph shown in Fig. 4.

The extended frequency range, in which the high accuracy of the large-scale transformation of the high voltage is preserved, is a consequence of the fact that the capacitances in the shielding circuit significantly shunt the parasitic capacitances of the shielding disks, and, moreover, the parasitic conductances of the shielding circuit and the parasitic conductances of the shielding disks on the surface, which are under a different potential, with increase proportionally in frequency. Accordingly, at high frequencies of the input voltage, parasitic inductances L1 – L4 and parasitic capacitances C9 – C11 remain the biggest factors affecting the accuracy of large-scale voltage conversion.

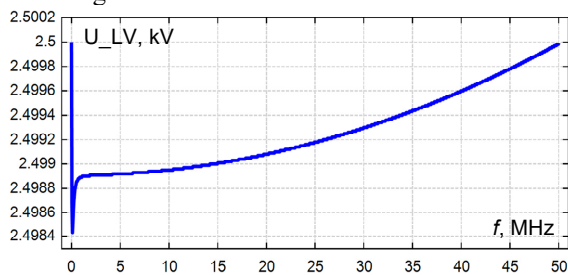


Fig. 4. Dependence of the voltage on the low-voltage arm of the voltage divider on the frequency at the capacitances in the shielding circuit of 10 nF in the range from 100 Hz to 50 MHz

In fact, if the specified parasitic inductances depend solely on the manufacturing technology of high-voltage precision resistors (or other lumped elements of the measuring circuit), the specified parasitic capacitances are dependent on the mutual spatial arrangement of the lumped elements of the measuring circuit and shielding disks. In Fig. 1 lumped elements have practically no parasitic capacitances on grounded surfaces and surfaces under a different potential. This situation is possible only if the ratio between the diameters of the shielding disks and the distance between them in height is significant, when the shielding practically excludes the ingress of external electric fields into the area of the location of the lumped elements of the measuring circle.

If we model mathematically and numerically calculate the spread of currents in the measuring and shielding circuits of a high-voltage divider (in codes using the finite element method) at frequency of 1 MHz (the front shape of a standard full lightning pulse, which is the fastest transient that is determined among the quality indicators of electricity, corresponds to a sinusoid with frequency of about 250 kHz) for the geometry of the electrodes and the nominal values of the lumped elements, according to which the simulation data obtained in the QUCS software package in Fig. 2 (without the use of shunt capacitors), it is possible to obtain results similar to those shown in Fig. 5.

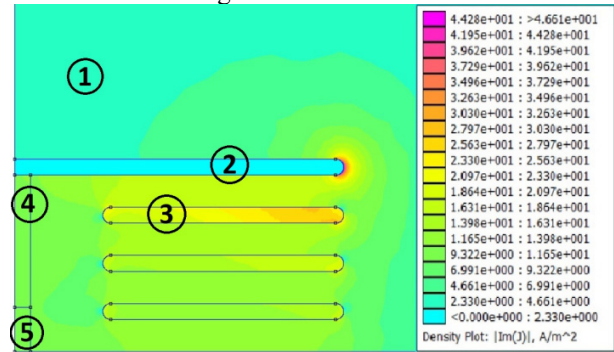


Fig. 5. The result of modeling the current density distribution in the mathematical model of the voltage divider, performed in the FEMM software package

Modeling in the FEMM software package was performed in an axisymmetric coordinate system by solving the equation derived from Maxwell system of equations:

$$-(\sigma + j\omega\epsilon_0\epsilon) \cdot \nabla^2 V = 0, \quad (3)$$

where  $\sigma$  is the conductivity of the medium;  $\epsilon$  is the relative dielectric permittivity of the medium;  $\omega$  is the angular frequency of the current;  $V$  is the electric potential.

In Fig. 5 the following are marked: 1 – the air region with relative dielectric permittivity  $\epsilon = 1$ ; 2 – the high-voltage electrode to which sinusoidal voltage with amplitude of 10 kV and frequency of 1 MHz is applied; 3 – the shielding disks; 4 – the active resistance of the high-voltage arm, modeled by a cylinder with geometry and conductivity that provide its resistance at constant voltage of 7.5 M $\Omega$ ; 5 – the active resistance of the low-voltage arm, modeled by a cylinder with geometry and conductivity that provide its resistance at constant voltage of 2.5 M $\Omega$ . The calculation area was limited to a spherical grounded surface with radius 10 times greater than the outer radius of the shielding disks. As a result of the unequal distribution of potentials in the measuring circuit (high-voltage and low-voltage arms) of the voltage divider and vertically along the end surfaces of the shielding disks, between the disks and the side surface of the resistors of the measuring circuit, a potential difference is formed, which, in the presence of parasitic capacitances, leads to the appearance of capacitive currents that increase with frequency of the applied voltage, which can be seen by the color distribution in Fig. 5. The maximum values of the capacitive current density correspond to the rounded end of the high-voltage electrode and are about 110 A/m<sup>2</sup>. At the same time, the integral values of the capacitive currents through the side surface of the resistor and through the horizontal surfaces of the shielding disks differ by a factor of ten at a frequency of 1 MHz (the current through the side surface

of the resistor is about 20 mA; the current through the horizontal surfaces of the shielding disks decreases with a decrease in the potential of the disk and, on average is about 400 mA). The presence of leakage of capacitive currents through the side surface of the resistors of the measuring circuit leads to the fact that the current that enters this circuit from the high-voltage electrode is not equal to the current that exits from the resistors of the low-voltage arm of the voltage divider to the grounded electrode. At the same time, the points on the side surface of the resistors of the measuring circuit, which correspond in height to the points closest to them on the surfaces of the shielding disks, have a higher potential for the resistor marked 4 in Fig. 5, and a lower potential for the resistor marked 5 in Fig. 5. As a result, through part of the side surface of the resistors of the measuring circuit, capacitive currents flow out, and through some areas - flow into the resistors. By ensuring the equality of the potentials of the shielding disks and their corresponding points on the side surfaces of the resistors of the active part, it is possible to quantitatively equalize the currents flowing in and out through the side surfaces of the resistors of the active part, in fact, getting rid of the influence of capacitive currents on the processes in the active part of the voltage divider.

**Mathematical modeling.** Calculation in the FEMM software package of the proposed mathematical model of the voltage divider allows obtaining the numerical values of the currents at the input to the resistor of the high-voltage arm and at the output of the resistor of the low-voltage arm by integrating the current density through the corresponding end surfaces of the resistors. Also, the simulation result allows to estimate the electric potential both on the surfaces of the shielding disks and on the side surfaces of the resistors of the active part.

The model according to Fig. 5 is constructed based on the outer radii of the high-voltage electrode and shielding disks of 100 mm. If the outer radii of the electrodes and disks are increased, leaving the distance between them unchanged, the capacitances of the shielding circle (between the shielding disks) will increase, and the parasitic capacitances of the shielding disks to the high-voltage electrode and to the grounded surfaces will remain almost unchanged. As a result, in the circuit in Fig. 1 capacitances C1 – C4 will increase, in accordance with (2). With significant capacitances in the shielding circuit, the current through this branch of the electric circuit will lead to an almost uniform distribution of potentials between these disks, as a result of which the ends of the shielding disks, which are close to the side surfaces of the resistors of the measuring circuit, will have potentials that are close to the potentials distributed over the surfaces of the resistors measuring circle. The same (or close to the same) distribution of potentials along the adjacent surfaces will lead to the fact that insignificant capacitive currents will flow through the parasitic capacitances formed by these surfaces (or the currents flowing from the side surface will be close to the currents flowing into this surface) due to a small potential differences. Of course, with significant values of the ratio of the outer radii of the shielding disks to the distance between them ( $R/d$ ), the parasitic capacitances of the side surfaces of the resistors of the measuring circuit to the grounded surfaces are so small, compared to the capacitances between the disks of the shielding circuit, that they can be neglected.

Table 1 shows the results of modeling in which the parameters of the model remained unchanged, in accordance with those specified for Fig. 5, except for the outer radii of the high-voltage electrode and the shielding disks, which were increased. The scale conversion error was indirectly determined through the difference between the currents that enter the active part of the measuring circuit from the end of the resistor, and that exit from it, in accordance with the expression:

$$\Delta = \frac{I_{HV} - I_{LV}}{I_{HV}} \cdot 100\% . \quad (4)$$

Table 1  
Results of modeling the influence of increasing radii of shielding disks on the value of parasitic capacitive currents in the measuring circuit

$R/d$	$I_{HV}$ , mA	$I_{LV}$ , mA	$\Delta$ , %
10	1,456	1,189	18,342
20	1,386	1,25	9,763
30	1,36	1,272	6,45
40	1,348	1,284	4,759
50	1,341	1,288	3,976
60	1,336	1,293	3,233
70	1,333	1,297	2,712
80	1,33	1,3	2,276
90	1,329	1,301	2,137
100	1,328	1,301	2,065
200	1,322	1,303	1,403
300	1,319	1,303	1,158

In Table 1, the current at the input to the high-voltage arm  $I_{HV}$ , the current at the output from the low-voltage arm  $I_{LV}$  and the difference  $\Delta$  between them in percent were determined.

The results of the calculations presented in Table 1 show that the percentage of parasitic capacitive currents decreases exponentially depending on the ratio of the outer radii of the shielding disks to the distances between them. However, it can also be seen that even at outer radii of the shielding disks of about 3 m, capacitive currents still account for about 1 % of the total current flowing in the measuring circuit. However, the manufacture of such sectioned structures of a high-voltage divider is not only unacceptable from the point of view of weight and size, but also practically impossible from the point of view of mechanical strength. In addition, since the shielding disks have a certain thickness that is proportional to the distance between adjacent disks, the end portions of the disks that are close to the side surfaces of the resistors of the measuring circuit have close to the same potential across the thickness of the ends, while the side surface of the resistor that is close to the inner ends of the shielding disks, has a potential distribution close to linear, which varies along the height corresponding to the thickness of the disk. As a result, even an infinite increase in the ratio  $R/d$  will not lead to a decrease in the leakage of capacitive currents to zero.

A simple design solution for the high-voltage arm of the voltage divider (this solution can also be applied to the low-voltage arm of the voltage divider) is to simultaneously increase the  $R/d$  ratio and reduce the thickness of the shield disks. This solution is described in [23]. The essence of the solution is that instead of sectioning the areas of the high-voltage arm with shielding disks with gas or liquid insulation between them, capacitance graded insulation with thin layers of solid (liquid, gaseous) dielectric and thin layers of

conductive foil between them should be used between the shielding disks. This structure of the insulation of the high-voltage arm of the voltage divider practically makes it impossible for external electric fields to penetrate into the area of the lumped elements of the measuring circuit of the voltage divider, as a result of which such a voltage divider becomes minimally sensitive to the parasitic capacitances of the structural components of the high-voltage arm to external objects and to neighboring sections.

Another advantage of using capacitance graded insulation between shielding disks is that the surface area of the electrodes on which charges are formed (the area of the ends of the electrodes), which create parasitic capacitances on external objects and neighboring structural elements of the high-voltage arm, is reduced. As a result, such capacitances are reduced, and the potential of the voltage applied to the divider is distributed more linearly vertically along the ends of the shielding disks and the ends of the conductive covers of the capacitance graded insulation (both externally and internally, near the lumped elements of the high-voltage arm). If it is necessary to increase the capacitance of the shielding circuit, it is easy to provide through cylindrical holes in the capacitance graded insulation, in which the lumped elements of the shielding circuit (parallel to the lumped elements of the measuring circuit) can be placed, which will also be shielded from the influence of external electric fields.

Since the measuring circuit of lumped elements between two adjacent shielding disks will be shielded by capacitance graded insulation, the distribution of potentials on the inner ends of which will be close to the voltage distribution along, for example, resistive elements of the measuring circuit, it becomes possible to unify individual segments of the high-voltage arm and create them separately manufactured blocks with electrically disconnected measuring and shielding circuits. Such modules can be connected in the future into a high-voltage structure designed for almost any voltage, similar to the arrangement of capacitor columns in capacitive voltage transformers (for example, NDE type). The low-voltage arm of such modular voltage dividers is better performed with a built-in analog-to-digital converter in order to get rid of the electrical connection between the primary and secondary circuits, as well as for convenient integration of such voltage dividers into digital control systems of substations and power facilities (Smart Grid).

**Verification of the mathematical model.** In order to verify the above-mentioned assumptions regarding the influence of the structure of the high-voltage arm of the voltage divider on its accuracy of large-scale high-voltage conversion, the mathematical model in Fig. 5 was changed. In the new model (Fig. 6), the distance between the shielding disks was increased, and capacitance graded insulation with copper covers 0.5 mm thick was placed between them (this thickness was chosen for reasons of reducing the volume of finite elements in the problem), as a dielectric material 2 mm thick fiberglass with relative dielectric permittivity of 5.5 was selected for capacitance graded insulation.

Also, the lumped elements of the high-voltage arm were represented by resistors in the form of cylindrical tubes (wall thickness 0.1 mm) with taps located one by one between adjacent shielding disks (film cylindrical

resistors with a bifilar shape of the conducting part on the side surface were modeled). The conductivity of the material of the resistors was chosen to ensure that a direct current of 1 mA flows through it.

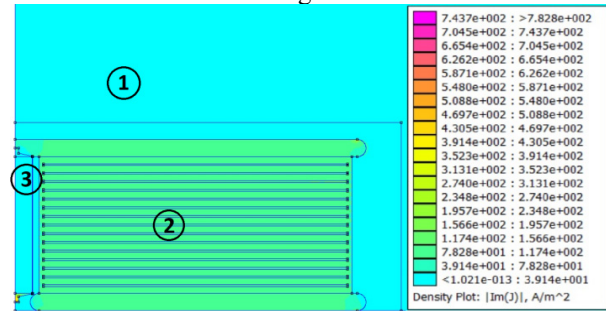


Fig. 6. The result of simulation of the density distribution of capacitive currents in the module with capacitance graded insulation of the high-voltage arm of the voltage divider at frequency of 1 MHz: 1 – area of air; 2 – area of capacitance graded insulation; 3 – resistor of the active part

On the high-voltage electrode of the mathematical model, the limiting condition of the potential of 10 kV was created. Due to the limitation of available computing power, the authors considered only 1 section of the voltage divider (one module) in the calculation. The distance from the side surface of the resistor of the active part to the inner end of the capacitance graded insulation was chosen in such a way as to ensure the smallest difference between the current entering the measuring circuit and the current leaving it. During the simulation, the radius of the hemispherical grounded surface, in the center of which the high-voltage arm of the voltage divider was simulated, was changed – from 3000 mm to 200 mm (in reality, when measuring high voltage, the distance from the voltage divider to grounded objects is much greater than the smallest value of the range). The currents at the input to the resistor of the high-voltage arm and the currents at the output of the resistor were determined by integrating the current density along the corresponding lines of the model based on the results of the numerical calculation, in accordance with (3).

The result of the simulation is a graph (Fig. 7) of the dependence of the current difference  $\Delta$  at the input and at the output of the high-voltage arm of the voltage divider, which determines the losses in the high-voltage arm, in accordance with expression (4), and which change with the change in the radius  $r$  of the grounded surface around the model.

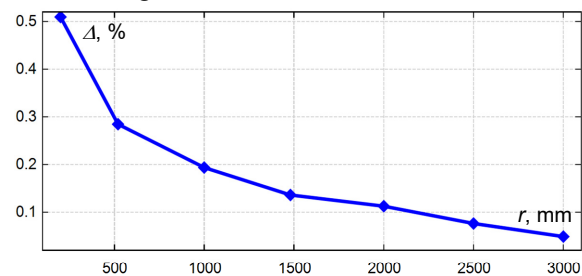


Fig. 7. Dependence of the difference in currents in the high-voltage arm of the voltage divider when the parasitic capacitances change on grounded surfaces (when changing the radius of the grounded surface) for current frequency of 1 MHz

**Analysis of results.** Analysis of the graph according to Fig. 7 shows the slowly increasing error of the scale transformation of the voltage divider in the range from 3000 mm to 200 mm radius of the grounded hemispherical surface around the model. Such a range can be considered a

very extended range, affecting stray capacitance changes that occur between shielding disks or capacitance graded insulation covers and grounded surfaces (in practice, grounded surfaces are not that close to voltage dividers).

When the radius of the grounded surface decreases, the non-uniform distribution of potentials along the inner ends of the capacitance graded insulation covers changes slowly, and therefore, the leakage currents from the lumped elements (resistors of the measuring circuit) of the active part through parasitic capacitances to the conductive surfaces of the shielding circuit change slightly. It should be noted that different areas of the side surfaces of the lumped elements (resistors) of the active part can be both surfaces of leakage of parasitic capacitive currents, and surfaces through which parasitic capacitive currents flow into these surfaces from the conductive surfaces of the shielding circuit, which are under a higher potential. The integral sum of inflowing and outflowing currents should approach zero with the same distribution of potentials along the surface of the resistor of the measuring circuit and along the inner ends of the capacitance graded insulation between the shielding disks. As an example of such a distribution of capacitive currents the graph (Fig. 8) can be considered, on which you can see the distribution of the density of currents flowing into the side surface of the resistor and currents flowing from this surface.

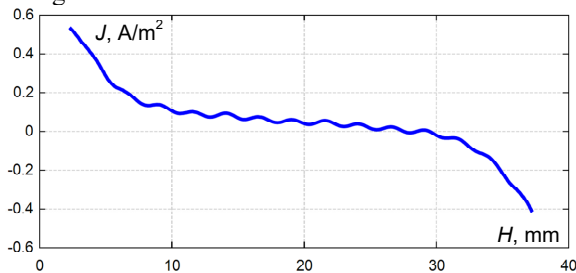


Fig. 8. Dependence of capacitive current density on lateral resistor surface on the height of the capacitance graded insulation covers (current frequency is 1 MHz)

In Fig. 8, it can be seen that the density of capacitive currents  $J$  changes non-linearly with an increase in the coordinate  $H$  according to the height of the side surface of the resistor, and at a height of about 25-30 mm, it changes its sign to the opposite. This means that in the lower part of the lateral surface of the resistor, capacitive currents flow into this surface, and in the upper part, they flow out (theoretically, it is possible to choose the location of the resistor in the model in such a way that the integrated capacitive currents flowing in and out of the resistor are equal to zero). The wavy shape of the dependence curve corresponds to the coordinates at the extremes of the vertical location of the ends of the capacitance graded insulation covers. Accordingly, an increase in the density of the arrangement of covers will lead to the leveling of such a curve.

However, the structural features of the section structure of the high-voltage arm of the voltage divider with real lumped elements (resistors) never make it possible to equalize such parasitic currents, only allow to reduce the difference between them to an acceptable value. But what is more important is not the reduction to zero of such a difference, but the stabilization of such a difference when changing the values of parasitic capacitances to grounded surfaces and surfaces under a different potential around the voltage divider. Increasing the total capacitance in the shielding circuit due to the arrangement of capacitors

parallel to the capacitance graded insulation (for example, in the cylindrical holes of the capacitance graded insulation, with inclusions between the shielding disks) allows to practically proportionally reduce the influence of external parasitic capacitances on the voltage distribution along the high-voltage arm for a wider range of input voltage frequencies. That is, in order for the high-voltage arm of the voltage divider, which consists of a large number of sections segmented by shielding disks (the same type of modules with capacitance graded insulation and an electrically disconnected section of the lumped elements of the measuring circuit), the distribution of potentials on the conductive surfaces close to the elements of the measuring circuit is still preserved more stable and uniform (and to get rid of the need for electrical connection of measuring and shielding electrical circuits on each segment or individual sections, which is characteristic of modern design solutions used in voltage dividers), it is necessary to increase the total capacitance of the sections of the shielding circuit of the corresponding segments (modules), to increase the number of layers of capacitance graded insulation between the shielding disks. Since such an increase in capacitance due to the geometric properties of the structural elements of the high-voltage arm modules, or due to the properties of the relative dielectric constant of the materials, has its limits, it is possible to increase the capacitance in the area of the shielding circuit only by adding lumped elements of a capacitive nature (capacitors) in parallel to the capacitance graded insulation. It is also possible to slightly (several times) increase the capacitance of the shielding circuit of the high-voltage arm of the voltage divider by increasing the outer radius of the shielding disks. An increase in the number of covers (a decrease in the thickness of the insulation between them) has a slight effect on the total capacitance of the high-voltage arm, but it significantly affects the uniformity of the potential distribution near the lumped elements of the measuring circuit (which can be seen by comparing the results of Table 1 and the graph in Fig. 7). It is also possible to reduce the influence of leakage of capacitive currents on the distribution of potentials on the lumped elements of the measuring circuit by reducing their resistance, but this will lead to an increase in heat losses in the active part, as a result of which the structure of the active part will be complicated and the stability of the voltage divider characteristics will deteriorate.

### Conclusions.

1. The existing design features of the structure of high-voltage dividers do not allow their use in open switchgears for the purpose of determining all power quality indicators due to the complex distribution of parasitic capacitances and inductances.
2. The division of the electric circuit of the high-voltage arm of the voltage divider into independent electric branches (measuring and shielding) makes sense only in the case when the total conductivity of the shielding branch is much higher and ensures the distribution of electric field potentials along the measuring branch is close to uniform.
3. By means of mathematical modeling, the dependence of the large-scale transformation error of the high-voltage divider on the geometric ratios of the structural elements of the shielding circuit was determined, which allows to vary the structure of the high-voltage arm of the voltage divider to expand the frequency range of the input voltage.

4. The analysis of the proposed mathematical model of the high-voltage divider proves the effectiveness of using the capacitance graded insulation voltage divider in the shielding circuit of the high-voltage arm of the voltage divider. At the same time, even at frequency of 1 MHz of the input voltage, the stability of the coefficient of scale transformation of the applied voltage is ensured with significant changes in the parasitic capacitances of the structural elements to external objects and to each other.

5. The application between the shielding disks of the high-voltage arm of the capacitance graded insulation allows to significantly reduce the effect on the large-scale voltage transformation coefficient of the parasitic capacitors on the grounded surfaces of the structural elements, and in addition, allows to switch to a unified sectioned structure of the high-voltage arm of the voltage divider, as a result of which the manufacture of voltage dividers can be carried out serially.

**Conflict of interest.** The authors of the article declare that there is no conflict of interest.

#### REFERENCES

- Anokhin Y.L., Brzhezitskiy V.O., Haran Ya.O., Masliuchenko I.M., Protsenko O.P., Trotsenko Ye.O. Application of high voltage dividers for power quality indices measurement. *Electrical Engineering & Electromechanics*, 2017, no. 6, pp. 53-59. doi: <https://doi.org/10.20998/2074-272x.2017.6.08>.
- Li D., Liu K., Lei M., Zhou F., Yue C., Yu J. Study on the ratio change measurement of 1000 kV HVDC divider based on improved DC voltage summation method. *High Voltage*, 2020, vol. 5, no. 2, pp. 202-208. doi: <https://doi.org/10.1049/hve.2019.0127>.
- Li D., Du B., Zhu K., Yu J., Liang S., Yue C. Optimization of DC Resistance Divider Up to 1200 kV Using Thermal and Electric Field Analysis. *Energy Engineering*, 2023, vol. 120, no. 11, pp. 2611-2628. doi: <https://doi.org/10.32604/ee.2023.028282>.
- Xie S., Mu Z., Ding W., Wan Z., Su S., Zhang C., Zhang Y., Xia Y., Luo D. Development of Broadband Resistive-Capacitive Parallel-Connection Voltage Divider for Resistant Voltage Monitoring. *Energies*, 2022, vol. 15, no. 2, art. no. 451. doi: <https://doi.org/10.3390/en15020451>.
- Zheng J., Li B., Zha K., Guo N., Wang L. Equipotential shielding voltage sensor for contact measurement of transient voltage in EHV/UHV power grids. *High Voltage*, 2021, vol. 6, no. 2, pp. 291-301. doi: <https://doi.org/10.1049/hve2.12016>.
- Galliana F., Caria S.E., Roccatò P.E. Towards a traceable divider for composite voltage waveforms below 1 kV. *Electrical Engineering*, 2022, vol. 104, no. 2, pp. 1121-1130. doi: <https://doi.org/10.1007/s00202-021-01368-5>.
- Kovacevic U.D., Stankovic K.D., Kartalovic N.M., Loncar B.B. Design of capacitive voltage divider for measuring ultrafast voltages. *International Journal of Electrical Power & Energy Systems*, 2018, vol. 99, pp. 426-433. doi: <https://doi.org/10.1016/j.ijepes.2018.01.030>.
- Thümmel T., Marx R., Weinheimer C. Precision high voltage divider for the KATRIN experiment. *New Journal of Physics*, 2009, vol. 11, no. 10, art. no. 103007. doi: <https://doi.org/10.1088/1367-2630/11/10/103007>.
- Shipu W., Wenlong P., Zhining Y., Kejie Z., Xixiu W. Study on the reliability of new kind of  $\pm 1$  100 Kv DC voltage divider under the action of impulse voltage. *The Journal of Engineering*, 2019, vol. 2019, no. 16, pp. 2575-2579. doi: <https://doi.org/10.1049/joe.2018.8815>.
- Havunen J., Hällström J. Reference switching impulse voltage measuring system based on correcting the voltage divider response with software. *IEEE Transactions on Instrumentation and Measurement*, 2021, vol. 70, pp. 1-8. art. no. 1006008. doi: <https://doi.org/10.1109/tim.2021.3063753>.
- Luo Y., Guo B., Qian B., Xu L., Zhang F., Li F., Feng X. Method to Evaluate the Resistance-Capacitance Voltage Divider and Uncertainty Analysis. *Energies*, 2021, vol. 14, no. 22, art. no. 7744. doi: <https://doi.org/10.3390/en14227744>.
- Jiang H., Pischler O., Schichler U., Havunen J., Hällström J., Merev A., Dedeoglu S., Özer S., Meisner J., Passon S., Gerdinand F. Prequalification of capacitors for high-precision voltage dividers. *22nd International Symposium on High Voltage Engineering (ISH 2021)*, 2021, pp. 309-314. doi: <https://doi.org/10.1049/icp.2022.0031>.
- Abdel Mageed H.M., Salah Eldeen R.S. Adapted Technique for Calibrating Voltage Dividers of AC High-Voltage Measuring Systems. *MAPAN*, 2020, vol. 35, no. 1, pp. 11-17. doi: <https://doi.org/10.1007/s12647-019-00334-8>.
- Lee S.H., Yu K.M., Choi J.Y., Jang S.M. Low-Uncertainty Equality Between the Voltage-Dividing and Resistance Ratio of a DC Resistive High Voltage Divider. *Journal of Electrical Engineering & Technology*, 2019, vol. 14, no. 4, pp. 1789-1795. doi: <https://doi.org/10.1007/s42835-019-00157-2>.
- Li Q., Wang L., Zhang S., Tang Y., Xu Y. Method to Determine the Ratio Error of DC High-Voltage Dividers. *IEEE Transactions on Instrumentation and Measurement*, 2012, vol. 61, no. 4, pp. 1072-1078. doi: <https://doi.org/10.1109/TIM.2011.2178672>.
- Hrbac R., Kolar V., Bartłomiejczyk M., Młcak T., Orság P., Vanc J. A development of a capacitive voltage divider for high voltage measurement as part of a combined current and voltage sensor. *Elektronika ir Elektrotechnika*, 2020, vol. 26, no. 4, pp. 25-31. doi: <https://doi.org/10.5755/j01.eie.26.4.25888>.
- Havunen J., Passon S., Hällström J., Meisner J., Schlüterbusch T.C. Empirical Characterization of Cable Effects on a Reference Lightning Impulse Voltage Divider. *IEEE Transactions on Instrumentation and Measurement*, 2023, vol. 72, pp. 1-9. doi: <https://doi.org/10.1109/TIM.2023.3276028>.
- Li B., He Y., Wang L., Cao M., Fu Z., Zhang H. Calibration Method of a Wideband AC Resistance Voltage Divider Based on an Equivalent Model. *Sensors*, 2023, vol. 23, no. 16, art. no. 7181. doi: <https://doi.org/10.3390/s23167181>.
- Pan Feng, Xiao Yong, Lin Guoying, Xiao Xia, Shuai Hang. Analysis of the influencing factors for the 500 kV DC voltage reference divider used for on-site calibration. *2015 12th IEEE International Conference on Electronic Measurement & Instruments (ICEMI)*, 2015, pp. 25-29. doi: <https://doi.org/10.1109/ICEMI.2015.7494180>.
- Boyko M.I., Syomkin S.O. Investigation of amplitude-temporal characteristics of a high-voltage resistive voltage divider. *Electrical Engineering & Electromechanics*, 2019, no. 4, pp. 59-68. doi: <https://doi.org/10.20998/2074-272X.2019.4.09>.
- Brzhezitskiy V.O., Haran Y.O., Trotsenko Y.O., Protsenko O.R., Derzhuk A.O., Dixit M.M. Ultimate effect of non-identity of resistive elements of high-voltage arm on frequency characteristics of broadband voltage divider (analytical research). *Electrical Engineering & Electromechanics*, 2023, no. 3, pp. 52-58. doi: <https://doi.org/10.20998/2074-272X.2023.3.08>.
- Brzhezitskiy V.O., Haran Y.O., Derzhuk A.O., Protsenko O.R., Trotsenko Y.O., Dixit M.M. Ultimate effect of non-identity of capacitive elements of high-voltage arm on frequency characteristics of voltage divider (analytical research). *Electrical Engineering & Electromechanics*, 2021, no. 4, pp. 46-52. doi: <https://doi.org/10.20998/2074-272X.2021.4.06>.
- Haran Y.O., Trotsenko Y.O., Protsenko O.R. *High-voltage wideband divider*. Patent UA, no. 155502, 2024.

Received 01.06.2024

Accepted 22.08.2024

Published 02.01.2025

Y.O. Haran<sup>1</sup>, PhD,  
Y.O. Trotsenko<sup>1</sup>, PhD, Assistant Professor,  
O.R. Protsenko<sup>1</sup>, PhD, Assistant Professor,  
M.M. Dixit<sup>2</sup>, Assistant Professor,

<sup>1</sup> National Technical University of Ukraine  
«Igor Sikorsky Kyiv Polytechnic Institute»,  
37, Prospect Beresteiskiy, Kyiv-56, 03056, Ukraine,  
e-mail: y.garan@kpi.ua (Corresponding Author)

<sup>2</sup> Vishwaniketan Institute of Management Entrepreneurship  
and Engineering Technology, India.

#### How to cite this article:

Haran Y.O., Trotsenko Y.O., Protsenko O.R., Dixit M.M. The impact of parasitic capacitances on the accuracy of scale transformation of high-voltage dividers. *Electrical Engineering & Electromechanics*, 2025, no. 1, pp. 65-72. doi: <https://doi.org/10.20998/2074-272X.2025.1.09>